PACS 61.82-BG; 81.40-WX

VARIATION OF COMPOSITIONAL CONTENT IN SUBSURFACE LAYERS OF HASTELLOY TYPE ALLOYS AS CAUSED BY MELT OF FLUORIDES ZrF_4 – NaF AND ELECTRON IRRADIATION

V.M. Azhazha, A.S. Bakai, Yu.P. Bobrov, A.N. Dovbnya, S.D. Lavrinenko, M.M. Pylypenko

National Science Center "Kharkov Institute of Physics and Technology", 1 Akademicheskaya St., 61108 Kharkov, Ukraine; E-mail: azhazha@kipt.kharkov.ua

The secondary-ion mass-spectrometry technique was employed to study the compositional content variation in subsurface layers of alloys of Hastelloy type that had been irradiated with electron beam with the average energy 9.6 MeV in the melt of sodium and zirconium fluoride salts at the temperature 650°C for 700 hours.

1. INTRODUCTION

The molten-salt reactors (MSR) are assumed to use the nuclear fuel in the form of fluoride melts opening the door for making continuous correction of the fuel content. As a rule, as fuel composition one uses the melt of fluorides of light and heavy elements of the type LiF, NaF, BeF_2, ZrF_4, ThF_4, in which are solved the fluorides of uranium or plutonium. The MSRs will use as their structural materials the nickel-based alloys of the type of Hastelloy N or their analogs [1-3].

This research was made on samples of alloys of the type of Hastelloy N, which had been cast from high-purity ingredient components at NSC KIPT.

The aim of this work was to make a study on the surface composition of high nickel-content alloys after their irradiation in the melt of sodium and zirconium fluorides at the temperature 650°C for 700 hours. The studies were made on samples, in which the values of deposited electron energy (E_{dep}) were 5,066 and 64 eV/atom.

2. MATERIALS AND RESEARCH METHODS

Samples of the high nickel-content alloys (alloys "A" and "B") were cast via the induction casting method in argon atmosphere out of high-purity components. The initial components were pre-refined, using various physical techniques. The purity of the initial components was as follows:

Nickel. The electrolytic nickel was used as the initial metal, cast over twice with the aid of electron beam melting (EBM). The refinement came out with a lower content of iron, cobalt, phosphorus, aluminum, magnesium, the content of arsenic, zinc, selenium and chlorine being decreased most substantially. The double EBM allowed us to produce nickel with the purity 99.994 wt.% [4].

Molybdenum. After the EBM the content of the metallic impurities came down by 10…30 times. Purification from silicon was very weak. The tungsten impurity is not removable from molybdenum. The principal purification is made from the gaseous impurities: oxygen, nitrogen and hydrogen.

Niobium. The initial casting material was niobium of the type NB-1. The metallic impurity content in it after the two consecutive EBM was as follows: Al – 0,004; Fe – 0,0001; Cr < 0,001; Ni < 0,0004; Si – 0,005; Cu – 0,0006; Ca < 0,003 wt.%.

Titanium. The initial casting material was titanium sponge TG-90. The EBM method was employed to produce a titanium ingot of the purity 99.99 wt.%.

Iron. The initial casting materials were rods of Armco-iron. The EBM of iron was made via droplet re-melting. The Brinelle hardness of the rods prior to the casting was 830 MPa, decreasing to 624 MPa after the refinement. The iron purity level is mainly determined by the content of nickel and cobalt.

Chromium. The major impurities in chromium are iron, silicon, aluminum, nickel and interstitial impurities: nitrogen, oxygen and carbon. The high-vacuum annealing of chromium samples made at the temperature 1,200°C for 5 hours brought down the content of the interstitial impurities by nearly ten times.

The content of the alloys: Ni – base, Mo – 11.7; Cr – 6.7; Ti – 0.47; Al – 0.83; Fe – 1.5; Mn – 0.5; Si – 0.15 wt.% (alloy "A"). The alloy "B" is different from the alloy "A" by having in it Nb substituted for Cr-0.5 wt.%, Y-0.05 wt.% added to the composition.

Samples of the alloys of Hastelloy type (alloys "A" and "B") were irradiated with electron beam with the average energy 9.6 MeV in the melt of sodium and zirconium fluoride salts at the temperature 650°C for 700 hours [6]. The evaluation of the electron energy (E_{dep}) deposited in the samples of the alloys indicated that its value was 5,066 and 64 eV per atom in the first and last (along the path of electron beam from linac) samples of the alloys, respectively [7]. For this reason, the studies on compositional variation of the alloy content in the subsurface layers were made, in the first place, on exactly those samples. The determination of the layer-by-layer elemental composition of the alloys was made, using the method of secondary-ion mass-spectrometry (SIMS) at the device MS-7201.

A schematic of the mass-spectrometer MS-7201 is given in Fig. 1. The analyzer includes a monopole rf-mass-spectrometer, a mass-analyzer, electronic optics and ion sources.

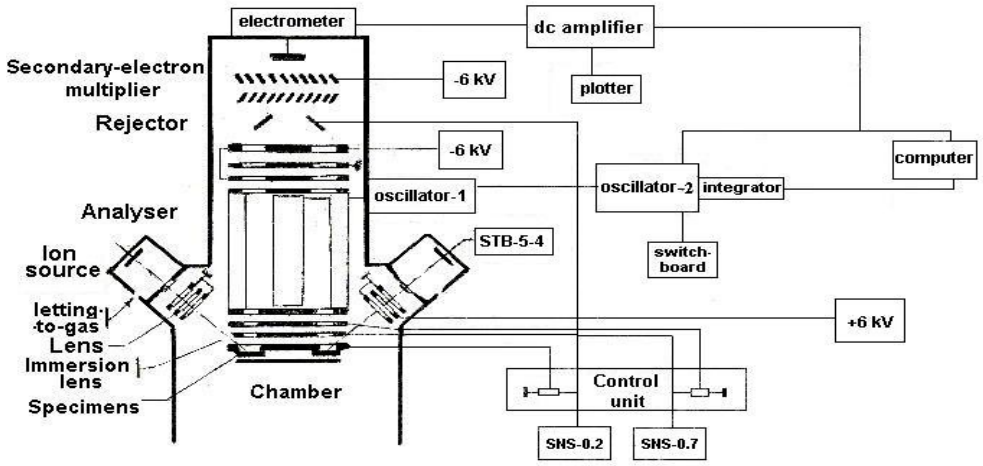

Fig.1. Schematic of mass-spectrometer

The underlying principle of the mass-spectrometer is based on the phenomenon of secondary ion emission. The primary ion beam, as it is injected from the ion source, bombards the sample analyzed, knocking out the secondary ions from the subsurface layers. The ions are collected with an immersion lens, the crossover of which is placed in the plane of the input aperture of the monopole that acts as a mass filter. The partial ion component, as it is released in the process of analysis from the integral ion beam, is separated in energies and transformed in the ion-electron converter into electron beam that is directed to the first dynode of the secondary-electron multiplier. The amplified electron current is fed to the DC amplifier, in which it is transformed into voltage. The high-frequency generator "oscillator-2" forms together with the unit "oscillator-1" the system of monopole rf-feeding that produces high-frequency voltage directed alongside with the appropriate DC voltage to the central monopole electrode. To recover ions of some mass, the high-frequency voltage amplitude at the monopole output varies smoothly across the respective range vs. control voltage value.

The registration system includes the secondary-electron multiplier, an electrometer, the DC amplifier and a laboratory-frame compensation recorder "LKS4-003". In the registration system, the voltage received at the electrometer input resistor is transformed in the DC amplifier into a signal that is convenient either for writing by the recorder "LKS4-003" or for further processing at the computer complex.

Performances:

- the range of analyzed mass numbers varies from 1 to 250 m/e;
- the resolution is not worse than 2.1 M if taken in the operation mode at the level of 50% of the intensity of mass-spectrum peaks;
- the primary ion beam current does not go below 5 μA;
- the primary ion beam diameter on the sample surface is not smaller than 4 mm.

The maximum registration time of the total mass-spectrum in the automatic mode must be as long as (30± 5) minutes.

The principal technical characteristics of the ion source are as follows: output on-sample ion current 5… 15 μA; discharge current, 2…4 mA; discharge glow voltage, 3…5 kV; working gas: hydrogen, argon or helium.

The alloys "A" and "B" after the irradiation in the fluoride melt were studied for the distribution of the main ingredients of Hastelloy-type alloys: nickel (mass 58), molybdenum (base isotope mass 98), chromium (mass 52), titanium (mass 48), aluminum (mass 27), the studies were also made on the fluoride melt base components, sodium and zirconium, into the depth of the sample. On each plate, the measurements were taken both from the surface layer facing the incident electron beam and from the reverse side.

The sample microstructure was examined at the optical microscope "MMR-4".

3. EXPERIMENTAL RESULTS AND ITS DISCUSSION

The typical SIMS spectrum picked up off the initial alloy sample is given in Fig. 2,a. The spectrum presents all the elements (including isotopes), which are included in its composition.

After the electron irradiation and exposure to the sodium and zirconium fluoride melt, the secondary ion spectrum, as taken off the sample surface, had the following characteristics peaks: 1 – sodium (mass 23) and satellite masses 39 and 40 (NaO, NaOH) that are proportional to the sodium peak value; 2 – peaks associated with zirconium isotopes with the masses 90, 91, 92, 94 and 96 and their satellites, for instance, mass 106 (which corresponds to the composition $^{90}Zr^{16}O$).

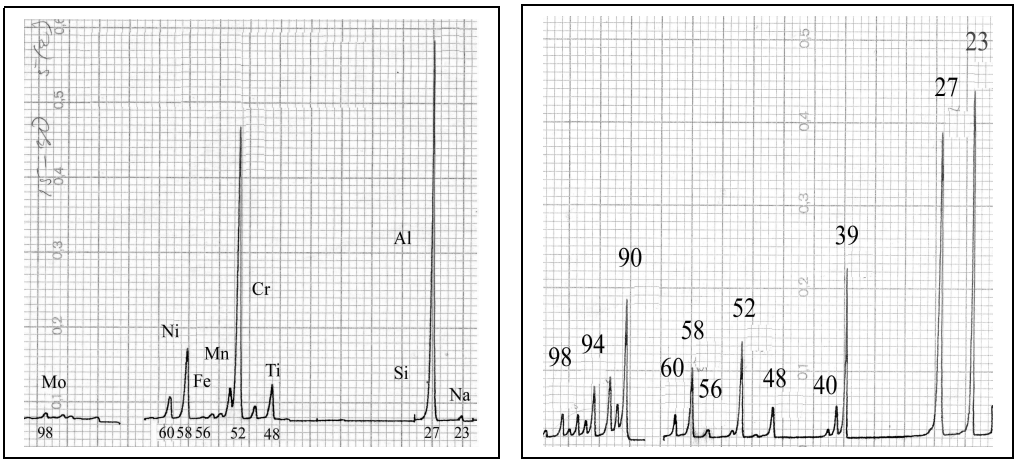

a *b*

Fig. 2. Typical secondary-ion spectrum picked up off Hastelloy-type samples (alloy "A"): a – initial; b – after exposure to the melt of sodium and zirconium fluoride salts at the temperature 650°C for 100 hours

In the further measurements, the isotope zirconium-90 (its percentage is 51.46%) was taken as the base one. Note that the spectrum showed an insignificant fluoride peak (mass 19). No registration was made of any peaks corresponding to the fluorides (NaF, ZrF_4). The mass-spectrum picked up off an alloy of the Hastelloy type after the corrosion test for 100 hours in the melt of sodium and zirconium fluorides is given in Fig. 3.

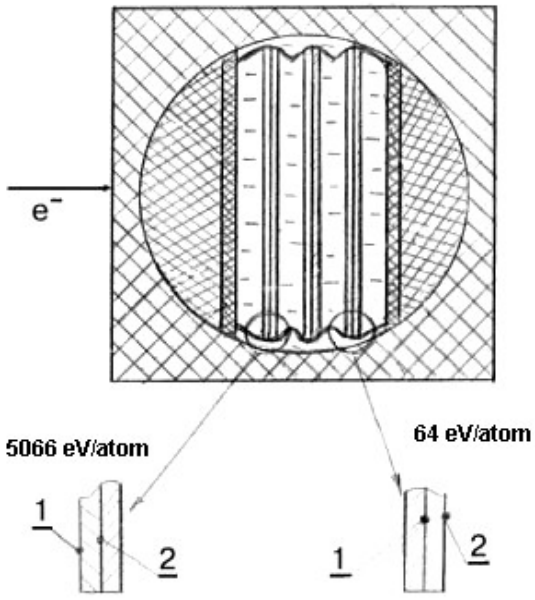

Fig. 3. Layout of disposition of samples of Hastelloy-type alloys in the ampoule relative to electron beam:
1 – surface facing electron beam, 2 – reverse side

Fig. 3 presents the layout of Hastelloy-type sample disposition in the ampoule relative to electron beam and place on the sample surface where the measurements were taken. The samples were positioned in pairs. The abutting between two adjacent samples was not tight so that the fluoride salt melt could penetrate between them and account for the corrosion processes.

Figures 4–9 show variation of the concentration of titanium, chromium, aluminum, iron, sodium and zirconium as measured in samples of the alloy "A" irradiated to different electron beam doses.

Titanium. The concentration of titanium in the alloy "A" increases at the depth of 10…15 microns from the surface, being especially high in the sample irradiated to the energy 64 eV/atom on the surface 2, see Figure 3. The sample of the alloy "B" irradiated to the high dose shows decreased titanium concentration in the surface layers of 5…10 microns.

Chromium. The samples of the alloy "A" show increased chromium concentration in the subsurface layer at the depth down to 15 microns. The samples of the alloy "B" irradiated to the dose 5,066 eV/atom show decreased chromium concentration at the depth of 10 microns.

Aluminum. In the samples of the alloys "A" and "B" irradiated to the large dose, the aluminum concentration decreases at the depth of 7…10 microns. The samples of the alloys "A" and "B" irradiated to the dose 64 eV/atom display (see Fig.3) increased aluminum concentration on the side 1 and decreasing of it on the side 2.

Iron. The samples of the alloys “A” and “B” show increased iron concentration on the surface down to the depth of about 5 microns. With increasing of the thickness of the layer removed, the concentration of iron is close to the initial one.

Sodium. The thickness of the layer, to which sodium penetrates in-depth of the alloys “A” and “B” is more than 20 microns after the irradiation to the dose 5,066 eV/atom. The samples of the alloy “A” irradiated to the dose 64 eV/atom show as well a negligible sodium saturation. As regards the samples of the alloy “B” that were irradiated to the smaller dose, sodium penetrates in-depth down to 10 microns.

Zirconium. The thickness of the layer, to which zirconium penetrates in-depth of the alloys “A” and “B” is more than 20 microns after the irradiation to the dose 5,066 eV/atom. As regards the alloys of the sample “B” that were irradiated to the dose 64 eV/atom, zirconium penetrates to the depth of up to 6 microns.

The microstructure of samples of the alloys “A” and “B” after the irradiation in the fluoride melt is given in Fig. 10.

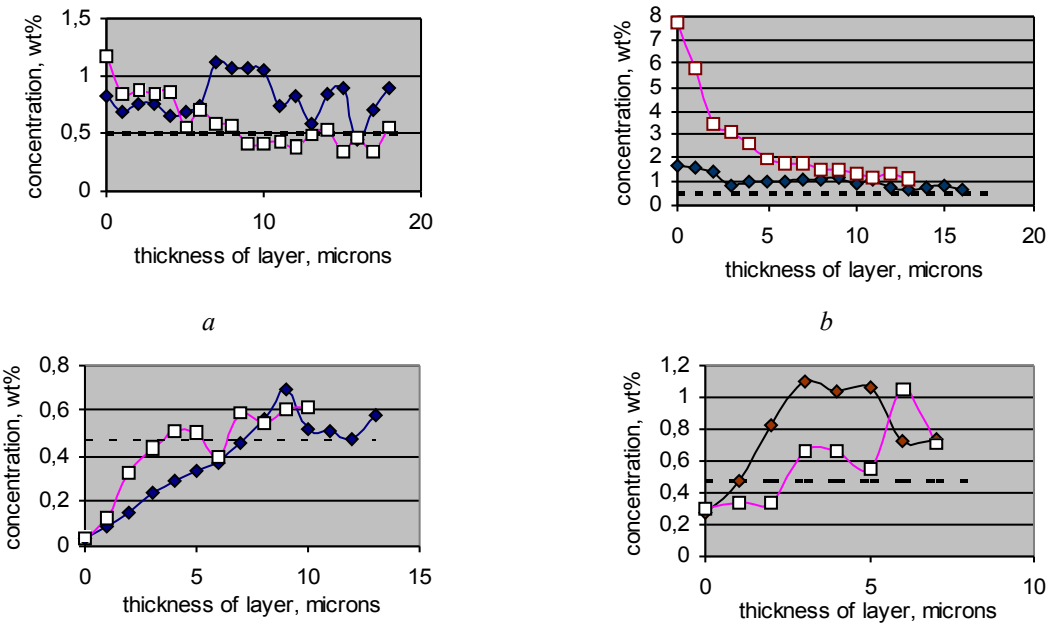

Fig. 4. Titanium concentration variation in samples of the alloys “A” (a,b) and “B” (c,d) irradiated to the doses: 5,066 (a, c) and 64 eV/atom (b, d):1-♦ - surface facing electron beam, 2-□ – reverse side, - - - initial concentration. The data of two consecutive measurements are connected with lines for the sake of convenient observation

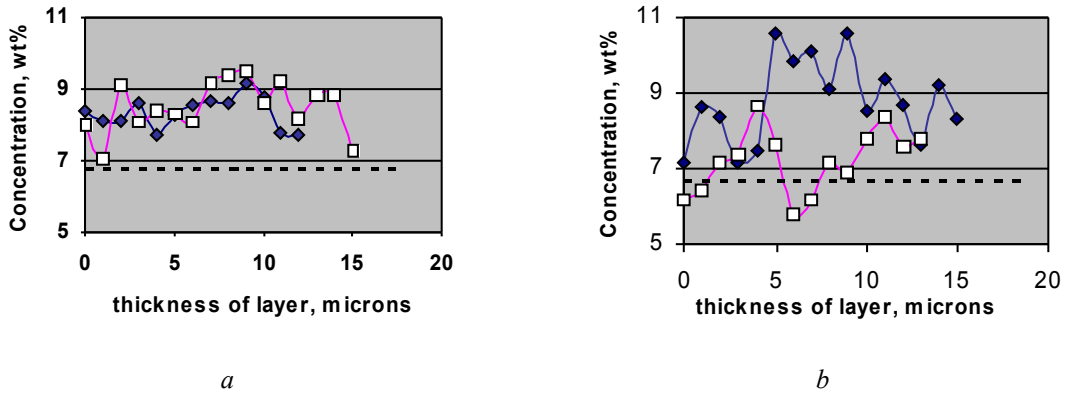

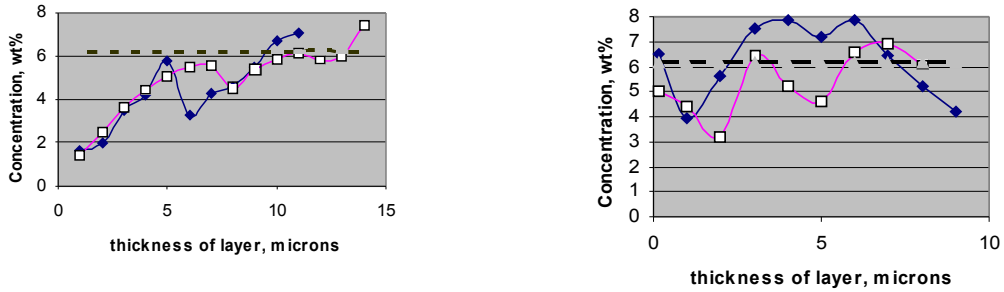

c *d*

Fig. 5. Chromium concentration variation in samples of the alloys "A" (a,b) and "B" (c,d) irradiated to the doses: 5,066 (a, c) and 64 eV/atom (b, d): 1-♦ - surface facing electron beam, 2-Î – reverse side, - - - initial concentration

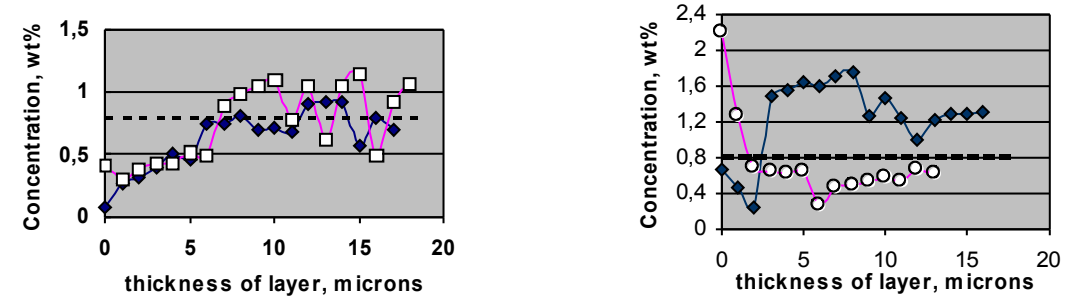

a *b*

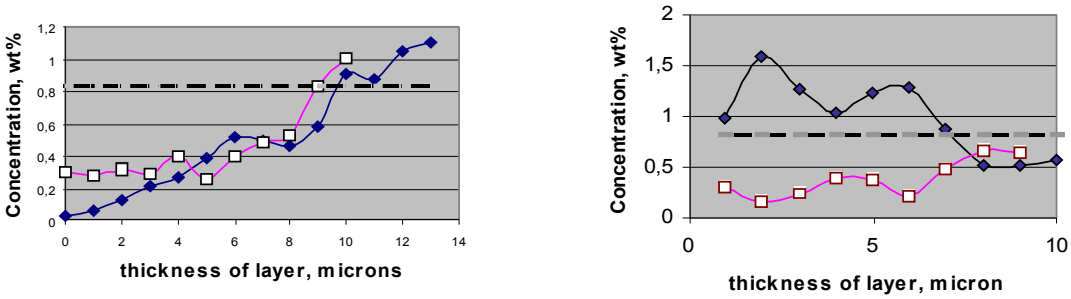

c *d*

Fig. 6. Aluminum concentration variation in samples of the alloys "A"(a,b) and "B" (c,d) irradiated to the doses : 5,066 (a, c) and 64 eV/atom (b, d): ♦ - surface facing electron beam, - reverse side, - - - - initial concentration

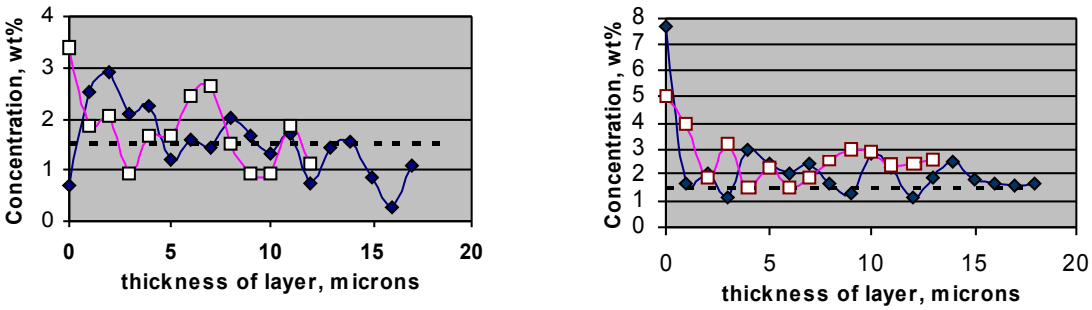

a *b*

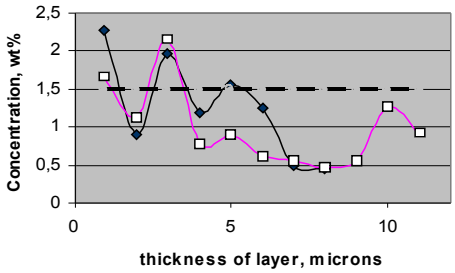

c

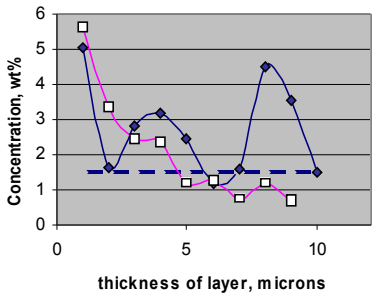

d

Fig. 7. Iron concentration variation in samples of the alloys "A" (a,b) and "B" (c,d) irradiated to the doses: 5,066 (a,c) and 64 eV/atom (b,d): ♦ - surface facing electron beam, - reverse side, - - - - initial concentration

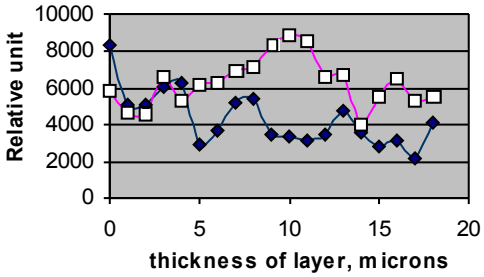

a

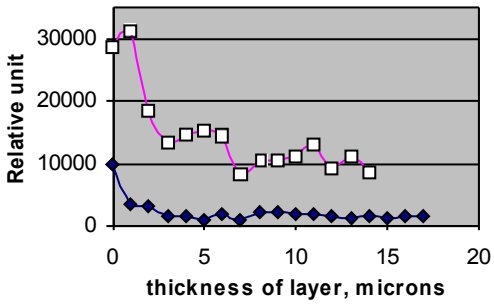

b

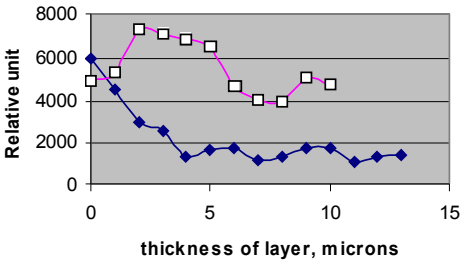

c

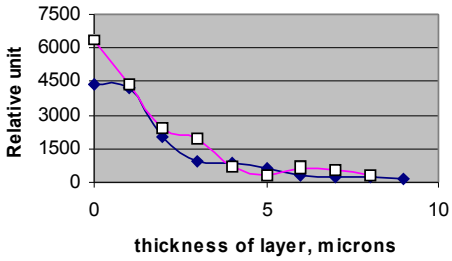

d

Fig. 8. Sodium concentration variation in samples of the alloys "A" (a,b) and "B" (c,d) irradiated to the doses: 5,066 (a,c) and 64 eV/atom (b, d) : ♦ - surface facing electron beam, - reverse side

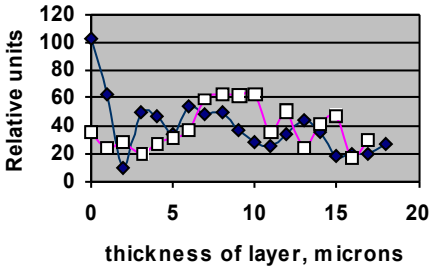

a

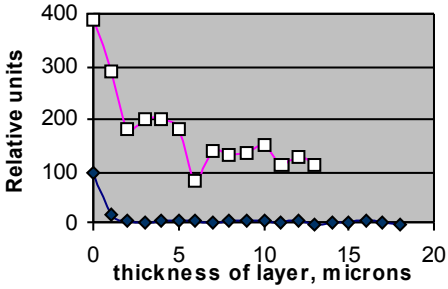

b

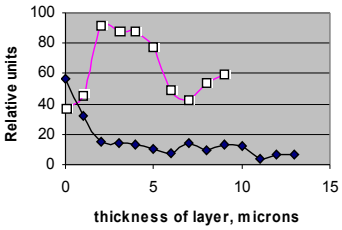

c

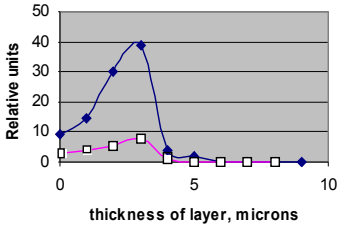

d

Fig. 9. Zirconium concentration variation in samples of the alloys "A" (a, b) and "B" (c, d) irradiated to the doses: 5,066 (a, c) and 64 eV/atom (b, d) : 1-♦ - surface facing electron beam, 2-Δ – reverse side, - - - initial concentration

One can see that the samples of the alloy "B" are characterized by lower values of the penetration of sodium and zirconium into the depth of the sample than it is the case with alloy "A". Decreasing of the irradiation dose acts to decrease the value of penetration of zirconium and sodium into the depth of the sample, yet it remains larger than in the non-irradiated samples. In all evidence, the migration of these impurities occurs along the grain boundaries, which is supported by examination of the sample surface morphology [8]. Notably, the corrosion of untightly abutting adjacent samples with a relatively low amount of the in-seeping molten salts does not differ much from the corrosion of the surfaces facing the melt. This observation implies that the chemical corrosion kinetics of the Hastelloy-type alloys in the salt melt under irradiation is controlled by the absorbed energy dose rather than by the volume and transport rate of the melt components in the near-surface layers.

4. CONCLUSIONS

1 The SIMS technique was used to study the distribution of sodium, zirconium, aluminum, chromium, iron, titanium in samples of the alloys of Hastelloy type of two compositions.

2. Samples of the alloy "A" after the irradiation to the dose of 5,066 eV/atom display depletion of the surface layer by aluminum to the depth of 7 microns. In the rest of the cases, enrichment is observable of the subsurface layers by titanium, chromium, iron.

3 The samples of the alloy "B" display after the irradiation to the dose of 5,066 eV/atom a decreased concentration of titanium, chromium, aluminum, iron in surface layers that are up to 10 microns thick.

4. The thickness of the layer, to which sodium penetrates into the depth of the samples of the alloys "A" and "B" is more than 20 microns after the irradiation to the dose of 5,066 eV/atom.

5. The samples of the alloy "B" are characterized by lower values of the penetration depth by sodium and zirconium into the bulk of the sample than it is the case with the alloy "A".

6. The chemical corrosion kinetics of the Hastelloy-type alloys in the salt melt under irradiation is rather controlled by the absorbed energy dose than the volume and transport rate of the melt components in the near-surface layers.

This work was supported in part by the STCU, Project #294.

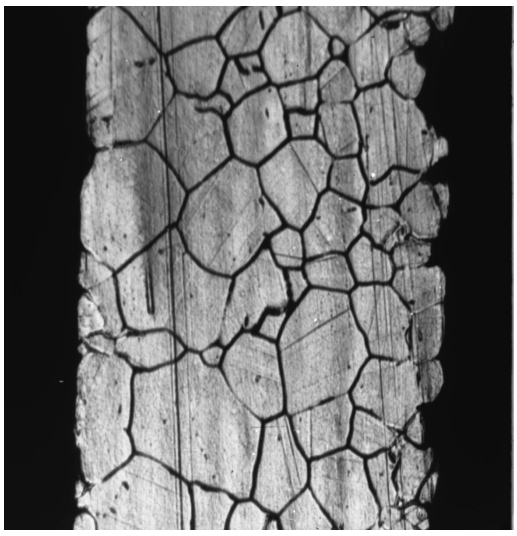

Alloy “A”. Irradiation dose is 5,066 eV per atom

Alloy “A”. Irradiation dose is 64 eV/atom

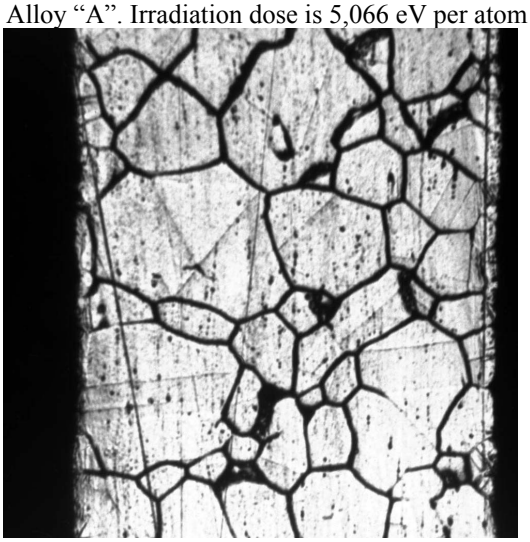

Alloy “B”. Irradiation dose is 5,066 eV per atom

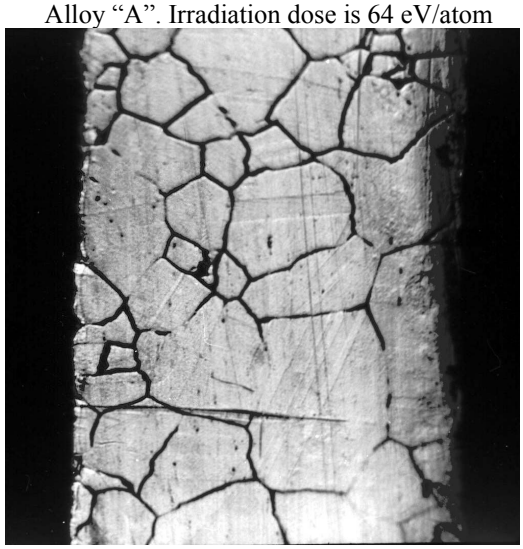

Alloy “B”. Irradiation dose is 64 eV per atom

Fig. 10. Microstructure of samples of the alloys “A” and “B” after irradiation. The electron beam was directed from the left. The sample width is about 300 microns

REFERENCES

1. V.L. Blinkin, V.M. Novikov. *Molten-salt nuclear reactors.* Moscow: “Atomizdat”, 1978, 112 p.

2. V.M. Novikov, V.V. Ignatyev, V.I. Fedulov, V.N. Cherednikov. *Molten-salt nuclear power plants: prospects and problems.* Moscow: “Energoatomizdat”, 1990, 192 p.

3. U.R. Grims. Problems of selection of materials for reactors with molten salts //*Materials and fuel for high-temperature nuclear power plants*. Moscow: “Atomizdat”, 1966, p. 69–98.

4. V.M. Azhazha, Yu.P. Bobrov, O.F. Vanzha, P.M. Vyugov, T.G. Yemlianinova, K.V. Kovtun, S.D. Lavrinenko, M.M. Pylypenko, V.I. Savchenko, A.D. Solopykhin, S.P. Stetzenko. Development of alloy for fuel cycle of molten-salt reactors //*Kharkov University bulletin. Series physical: “Nuclei, particles, fields”*, N 619, issue 1(23), 2004, p. 87–93.

5. V. Azhazha, A. Bakai, S. Lavrinenko, Yu. Bobrov et al. Alloys for molten-salt reactors // *Proc. XVI Int. Conf. On Physics of Radiation Phenomena and Radiation Materials Science, September 6-11,* 2004, Alushta, the Crimea, p. 271–272.

6. V.M. Azhazha, A.S. Bakai, V.A. Gurin, A.N. Dovbnya, N.V. Denidov, A.I. Zykov, E.S. Zlunitsyn, S.D. Lavrinenko, L.K. Myakushko, O.A. Repikhov, A.V. Torgovkin, B.M. Shirokov, B.I. Shramenko. Radiation test stand for testing of structural materials in simulation of molten-salt reactor //*Book of Abstracts, XVI Int. Conf. On Physics of Radiation Phenomena and Radiation Materials Science, September 6-11,* 2004, Alushta, the Crimea, p. 270.

7. A.S. Bakai, M.I. Bratchenko, S.V. Dyuldia. Modeling of electron beam absorption profiles in simulative experiments on studies of radiation resistance of Hastelloy in the ambience of molten fluorides //*Book of Abstracts, XVI Int. Conf. On Physics of Radiation Phenomena and*

Radiation Materials Science, September 6-11, 2004, Alushta, the Crimea, p. 274–275.

8.V.M. Azhazha, A.S. Bakai, A.N. Dovbnya, K.V. Kovtun, S.D. Lavrinenko, D.G. Malykhin, M.M. Pylypenko, V.I. Sachenko, N.A. Semyonov, S.V. Strigunovsky, B.I. Shramenko //*Book of Abstracts, XVI Int. Conf. On Physics of Radiation Phenomena and Radiation Materials Science, September 6-11*, 2004, Alushta, the Crimea, p. 276–277.

ИЗМЕНЕНИЕ КОМПОЗИЦИОННОГО СОСТАВА В ПРИПОВЕРХНОСТНЫХ СЛОЯХ СПЛАВОВ ТИПА ХАСТЕЛЛОЙ Н ПОД ДЕЙСТВИЕМ РАСПЛАВА ФТОРИДОВ ZrF_4 – NaF И ЭЛЕКТРОННОГО ОБЛУЧЕНИЯ

В.М. Ажажа, А.С. Бакай, Ю.П. Бобров, А.Н. Довбня, С.Д. Лавриненко, Н.Н. Пилипенко

Методом вторично-ионной масс-спектрометрии исследовано изменение композиционного состава в приповерхностных слоях образцах сплавов типа Хастеллой, облученных пучком электронов со средней энергией 9,6 МэВ в расплаве солей фторидов натрия и циркония при температуре 650°С в течение 700 ч.

ЗМІНА КОМПОЗИЦІЙНОГО СКЛАДУ В ПОВЕРХНЕВИХ ШАРАХ СПЛАВІВ ТИПУ ХАСТЕЛОЙ Н ПІД ДІЄЮ РОЗПЛАВУ ФТОРИДІВ ZrF_4 – NaF І ЕЛЕКТРОННОГО ОПРОМІНЕННЯ

В.М. Ажажа, О.С. Бакай, Ю.П. Бобров, А.М. Довбня, С.Д. Лавриненко, М.М. Пилипенко

Методом вторинно-іонної мас-спектрометрії досліджено зміну композиційного складу в приповерхневих шарах зразків сплавів типу Хастелой, опромінених пучком електронів з середньою енергією 9,6 МеВ в розплаві солей фторидів натрію і цирконію при температурі 650°С протягом 700 г.